

## Cluster formation and atomic intermixing at the reactive V/Ge(111) interface

M. del Giudice, J. J. Joyce, M. W. Ruckman, and J. H. Weaver

*Department of Chemical Engineering and Materials Science, University of Minnesota, Minneapolis, Minnesota 55455*

(Received 20 March 1985)

A detailed low-energy electron-diffraction, synchrotron-radiation, and resonance-lamp photoemission-spectroscopy study of the reactive V/Ge(111) $2\times 1$  interface is presented. High-resolution core-level and valence-band results indicate the formation of vanadium islands for coverages  $\Theta$  less than  $\sim 2 \text{ \AA}$  (average radius  $\sim 20 \text{ \AA}$ , number density  $\sim 10^{12} \text{ cm}^{-2}$ ). Core-level decomposition makes it possible to then follow the growth and attenuation of each Ge species. In particular, disruption of the substrate occurs above  $\sim 2 \text{ \AA}$  and an intermixed V-Ge region forms. This reacted region is ultimately covered up for  $\Theta \geq 20 \text{ \AA}$ , but strong out-diffusion of Ge allows the formation of a more V-rich species up to  $\sim 80 \text{ \AA}$ . Beyond  $\sim 80 \text{ \AA}$ , Ge out-diffusion is significantly reduced and a pure vanadium overlayer forms. Evolution of the Schottky-barrier height variation was monitored through binding-energy changes for the Ge  $3d$  core level and, although the Schottky-barrier height  $\Phi_b$  was completely developed by  $\sim 2 \text{ \AA}$ , a slow increase of  $\Phi_b$  was observed as a secondary effect of atomic intermixing ( $\sim 0.05 \text{ eV}$  after  $10 \text{ \AA}$ ).

### I. INTRODUCTION

For the last decade or so, major efforts have focused on the microscopic properties of metal-semiconductors interfaces and how they influence the macroscopic properties of the junction.<sup>1,2</sup> Nonetheless, Ohmic contacts and microelectronic devices are still being built using empirical prescriptions—from which we conclude that our basic understanding of this very complex problem is far from complete. In this context, both reassessments of the large amount of information already available and wider, systematic studies of metal-semiconductor interfaces are in order. At issue are questions related to adatom clustering on surfaces and their role in intermixing and Schottky-barrier formation,<sup>3–5</sup> atomic intermixing and local bonding configurations at an interface,<sup>6</sup> and the influence on the reaction kinetics of defects and impurities present at semiconductor surfaces.<sup>7,8</sup>

The increasing interest in refractory-metal-semiconductor interfaces is connected to both their technological applications and to fundamental scientific properties related to interaction between  $sp^3$  semiconductors and  $d$ -band metals.<sup>9–12</sup> In this paper we report a study of one of these interfaces, V/Ge(111) $2\times 1$ . Germanium was chosen because high-resolution Ge  $3d$  core-level information could be used to follow the evolution of the interface in a very detailed way. Indeed, by performing Ge  $3d$  line-shape decomposition it was possible to characterize the different Ge environments which form and to follow the relative concentration of each during the growth of the interface. Results presented here suggest adatom aggregation at low coverages before the onset of reaction, followed by the formation of an inherently heterogeneous interface. They also show that significant Ge out-diffusion occurs to very high coverage although the primary reacted region is completed after  $\sim 20 \text{ \AA}$  of vanadium deposition.

### II. EXPERIMENTAL TECHNIQUES

The photoemission studies were done at the Synchrotron Radiation Center's Tantalus light source using the 3-m toroidal grating monochromator and the grazing incidence "Grasshopper" monochromators and in our laboratory at the University of Minnesota using a helium resonance lamp. Primary studies of the Ge  $3d$  core levels were conducted at  $h\nu=40, 50,$  and  $75 \text{ eV}$  in order to vary the surface sensitivity of the measurements. The valence-band studies were conducted using photon energies of 50 to 21.2 eV to enhance, respectively, the V  $3d$  and the substrate emission. The valence bands were recorded with an overall resolution of 300 meV for  $h\nu=50 \text{ eV}$  and 170 meV for  $h\nu=21.2 \text{ eV}$ . A very detailed study of the V/Ge behavior in the low-coverage regime ( $\Theta \leq 2 \text{ \AA}$ ) examined the Ge  $3d$  core emission with an overall resolution of 200 meV. This high-resolution study made it possible to distinguish *three* different core-level components and to determine their binding-energy variations and line-shape changes. We estimate a reproducibility of the relative position of the different components within 0.05 eV.

Both of the photoemission spectrometers operated with a collection geometry having the photon beam incident on the sample at about  $45^\circ$  ( $s$ -polarized light for synchrotron radiation, unpolarized light for resonance lamp) and the surface normal directed into the collection annulus of the cylindrical mirror analyzer (CMA).<sup>13</sup> Low-energy electron diffraction (LEED) and resonance-lamp photoemission studies were conducted in parallel in order to correlate electronic evolution with structural modification of the interface using the same sample. Ge crystals ( $n$  type with Sb dopant, 5–10  $\Omega \text{ cm}$ ) oriented along the [111] direction were cut to give dimensions  $\sim 4\times 4\times 20 \text{ mm}$ . These posts were notched, etched, and finally cleaved *in situ* to obtain Ge(111) $2\times 1$  surfaces. The quality of each cleave was checked with valence-band and core-level

photoemission and, when possible, with LEED to assure a well-defined  $2 \times 1$  reconstruction. Evaporation of V films was performed using a resistively-heated 5-mil Mo boat and required 100–110 A from a regulated power supply. The operating pressure of each experimental chamber was mid- $10^{-11}$  Torr and evaporations were always done at pressures better than  $2 \times 10^{-10}$  Torr. Extended degassing of the V source was necessary to obtain such low pressures but was essential to obtain contamination-free V surfaces. The rates of evaporation were determined using a quartz thickness monitor. Every coverage was obtained by first stabilizing the evaporation rate at 1 Å/min prior to exposing the sample to the V source (source-to-sample distance  $\sim 30$  cm). All of the studies reported here were conducted at room temperature. The results are representative of many cleaves and repetitive evaporation cycles. In this paper we use angstrom units where  $1 \text{ Å} = 0.95$  monolayer (ML)  $= 6.95 \times 10^{14}$  atoms/cm<sup>2</sup>.

### III. EXPERIMENTAL RESULTS

In Figs. 1 and 2 we report results which show the behavior of the Ge 3*d* core emission at the V/Ge interface taken at two different photon energies (40 and 50 eV) with different surface sensitivities ( $\lambda \sim 20$  and 10 Å, respectively).<sup>14</sup> Analogous results were obtained at 75 eV with

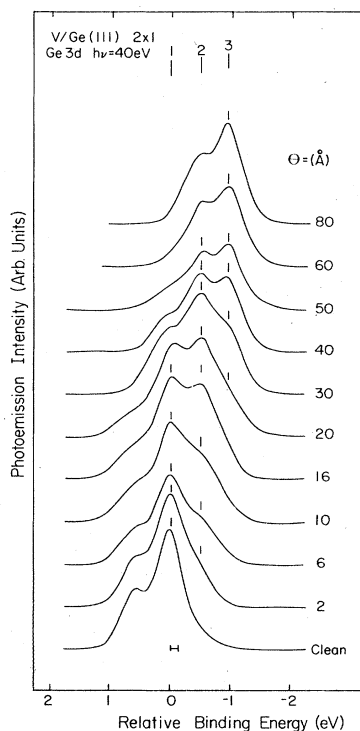


FIG. 1. Core-level results for the Ge 3*d* core at  $h\nu=40$  for V overlayers after the subtraction of inelastic background. The tick marks indicate the relative binding-energy position for the substrate (1), the intermixed (2), and the segregated (3) species. The substrate emission is present up to  $\sim 20$  Å of V coverages. Results are corrected for a band bending of 125 MeV (bottom-most line).

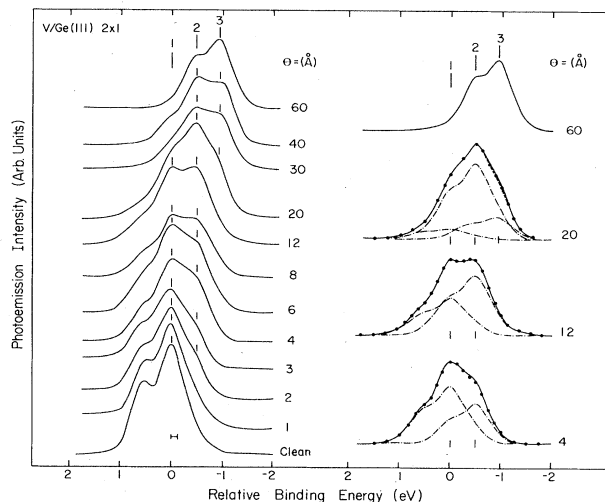


FIG. 2. Ge 3*d* core-level EDC's as in Fig. 1 but with greater surface sensitivity ( $h\nu=50$  eV). Again, three distinct species can be identified. On the right-hand side we show line-shape decompositions for  $h\nu=50$  eV and for different overlayer thickness. The core EDC's could be fit with three doublets for all coverages greater than  $\sim 2$  Å, allowing only the relative amounts of components 1, 2, and 3 to vary.

higher surface sensitivity but poorer energy resolution. In Fig. 3 we show high-resolution results in the ultralow-coverage range 0–2 Å. In each figure the bottom energy distribution curve (EDC) is for the clean surface, and EDC's offset vertically reveal the evolution characteristic of the interface. The energy scales have been corrected to compensate for changes in the Fermi-level position. The initial band bending of 125 meV was achieved by 2 Å, as indicated by the horizontal line. Further metal deposition reversed this band-bending trend, and the features rigidly shifted to lower binding energy as determined from the trailing edge of the bulk Ge 3*d* core emission. In the data presented, this shift is also taken into account and will be discussed in subsequent paragraphs.

The Ge 3*d* core EDC's show gradual changes in shape for  $0 \leq \Theta \leq 2$  Å, as shown in Fig. 3. This is consistent with line-shape broadening due to weak but non-negligible interaction of V atoms with the substrate and with the structural relaxation for  $2 \times 1$  to  $1 \times 1$ . Analogous broadening was reported for the Ag/Ge system for which no intermixing was observed.<sup>15</sup> Indeed, we find no evidence of a reacted Ge component until the overlayer coverage exceeds  $\sim 2$  Å. Above 2 Å, the new component, which is shifted  $\sim 0.5$  eV to lower binding energy, grows and can be observed up to 50–60 Å of nominal film thickness (see tick marks in Figs. 1–3). For  $\Theta > 20$  Å, a third, fully-shifted component appears at 0.95-eV lower binding energy relative to the unreacted component. This then dominates until  $\Theta > 80$  Å when the intensity of the Ge 3*d* core emission drops, indicating that the reacted region serves as a barrier for subsequent out-diffusion of Ge atoms. We can then identify three distinct regimes of interface formation based on the appearance of the Ge 3*d*

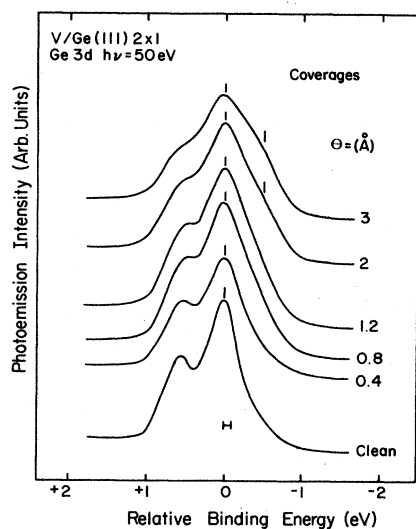


FIG. 3. High-resolution results for Ge 3d cores at  $h\nu=50$  eV at low V coverages. As shown by tic marks, the component associated with the formation of an intermixed layer starts to form clearly at  $\sim 2$  Å. A continuous broadening is also observed at lower coverage (see discussion in text). The bottom line shows the total amount of the band bending.

cores. The first corresponds to a weakly interacting regime, the second to an intermixed V/Ge phase, and the third to covering up of the V/Ge overlayer.

On the right-hand side of Fig. 2 we present representative line-shape analysis results for the Ge 3d core EDC's. To obtain these decompositions, we used empirically-fit doublets shifted by 0.5 and 0.95 eV relative to the substrate component with spin-orbit splitting of 0.6 eV and branching ratios of 0.61 ( $h\nu=50$  eV). It is important to note that every Ge 3d EDC for  $\Theta \geq 2$  Å could be fit in this way by varying only the relative intensity of the components, each one located at a fixed position in binding energy and corresponding to well-defined configurations for the Ge/V atoms. With these results it will be possible in the next section to semiquantitatively model the interface chemical and atomic distribution.

In Figs. 4 and 5 we show the valence-band modifications induced by successive depositions of V onto Ge(111)2x1 for photon energies of 50 and 21.2 eV, respectively. The bottom EDC in each figure is for the clean, cleaved Ge(111)2x1 surface. The feature denoted by *D*, which is Ge derived and has minimal overlap with V derived states, has been used to align the spectra at low coverages in both figures. The low coverage EDC's (0–2 Å) in Fig. 5 are normalized to the emission of clean Ge(111) and show little change in Ge features beyond steady attenuation. At the same time, difference curves reveal the growth of V 3d emission within 2–2.5 eV of the Fermi level (not shown). The growth of these V-induced states is particularly evident from Fig. 4 because spectra at  $h\nu=50$  eV emphasize the V character and because of the enhanced surface sensitivity at that energy. There, the shaded region highlights the changes between the clean surface and the 0.5-Å covered surface.

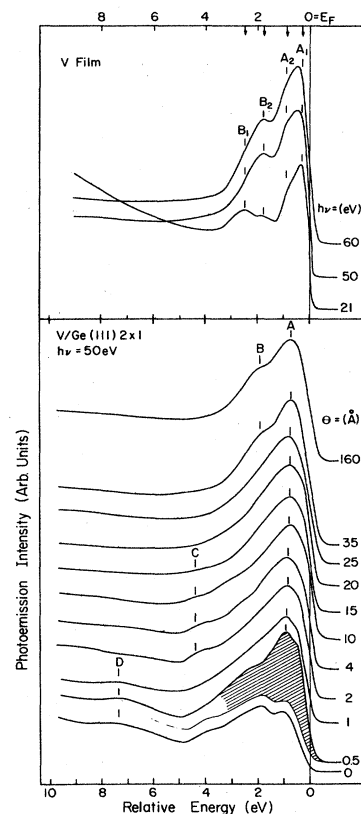


FIG. 4. Valence-band EDC's for V overlayers with  $h\nu=50$  eV. The feature denoted by *D* was used to align the low-coverage spectra. The presence of a reacted species for  $\Theta \geq 2$  Å is reflected by peak *C*. For  $\Theta \geq 35$  Å, the spectra converge to bulk V with the splitting of the *d* bands into two features labeled *A* and *B*. The shaded area represents the difference between the clean Ge EDC and the one at 0.5 Å of V coverage. The upper panel shows the V *d* bands at different energies with high resolution for a thick V film.

As the *d* bands grow, the main feature labeled *A* narrows and shifts to 0.3 eV below  $E_F$  (total shift of 0.5 eV between 3 and 100 Å as measured at 21.2 eV). The weak structure denoted by *C* about 4.5 eV below  $E_F$  persists to  $\sim 25$  Å and is related to states of the V-Ge reacted phase. Its disappearance and the growth of peak *B* at about 2.2 eV correspond to the onset of the third interface growth regime identified from the core results as the covering-up regime. Finally, the valence band (VB) evolves slowly to that of metallic vanadium such that by  $\sim 80$ -Å coverage the convergence is complete, as judged by the 21.2-eV spectra.

At the top of Fig. 4 we report VB spectra for a thick film of V at  $h\nu=2.12$ , 50, and 60 eV with  $\sim 200$ -meV total resolution for 21.2 and 50 eV. From these spectra it can be seen that structures *A* and *B* identified in the evolving interface ultimately split into four features which can be related to the band structure ( $A_1$  at 0.3 eV,  $A_2$  at 0.9 eV,  $B_2$  at  $\sim 1.8$  eV, and  $B_1$  at  $\sim 2.5$  eV). At 21.2 and 50 eV we are, respectively, near the minimum and the maximum for the photoionization cross section for *d*

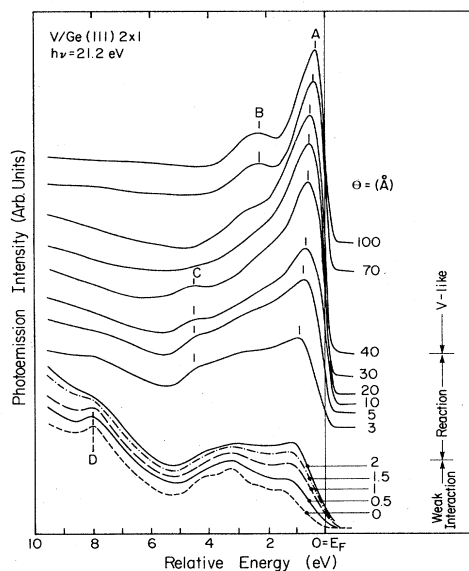


FIG. 5. Representative EDC's showing the effect of increasing V coverage for  $h\nu=21.2$  eV. The valence-band spectra from the intermixed V/Ge species ( $2 \leq \Theta < 20$ ) show a well-defined structure at 4.5 eV below  $E_F$  (peak C). The increasing emission at 2.2 eV (peak B), together with a sharpening of the feature A, marks the convergence to a V-like valence band that occurs for  $\Theta \geq 40$  Å of coverage.

states.<sup>16</sup> We can then emphasize the *d* character of the VB states, and we see that the main *d* contribution comes from the states around  $A_2$  and  $B_2$ . Insight into the origin of these features, particularly with regard to their angular momentum character, can be gained through comparison with band calculations.<sup>17,18</sup> The experimental structure at  $-0.3$  eV appears to be a superposition of *p* and *d* states related to the  $\Sigma$  pocket. Moreover, the *d*-derived density of states (DOS) is consistent with the energy location of experimental peaks  $A_2$  and  $B_2$  with more mixed angular momentum character for the peak closest to  $E_F$ .

The results presented in Figs. 1–5 emphasize the changing Ge environment and its correlation to changes in the valence-band structures. These results all point to the existence of several well-defined V/Ge interface regimes. In the following we discuss those results and use them to model the evolving interface.

#### IV. DISCUSSION

##### A. Low-coverage region ( $0 < \Theta < 2$ Å)

Studies in the low-coverage region allow us to characterize the initial stage of interface formation, identify ordering or the lack of overlayer ordering, determine the onset of reaction, and examine the driving forces of interface reactions.

Previous work with metal-semiconductor interfaces have shown that metal overlayers can exhibit a number of different structural morphologies.<sup>1,3,6,10,15,19</sup> The growth

modes for this kind of interfaces include layer-by-layer (Frank–van der Merve), three-dimensional islanding (Volmer–Weber), and island growth over a monolayer (Stranski–Krastanov) behaviors. Careful analysis of the results of our low-coverage core-level studies makes it possible to model the growth of V on Ge prior to the onset of reaction. It should be clear, however, that the overlayer is inherently metastable since reaction is triggered at  $\sim 2$ -Å coverage.

In Fig. 3 we report some of the core-level EDC's recorded at 50 eV with a measured overall resolution of 200 meV, i.e., much less than the observed broadening of the Ge 3*d* doublets [0.5 eV full width at half maximum (FWHM)] so that it is possible to determine variations in FWHM (line-shape broadening) indicative of charge redistribution. As shown, the first clear evidence of a shifted component appears at 2 Å, but a continuous broadening of the doublet is observed as the V coverage is increased from 0 to 2 Å. Analogous results were obtained at 75 eV with greater surface sensitivity but with lower overall resolution. Any attempt to fit these spectra by varying the intensity of the doublet associated with the reacted species was unsuccessful up to 2 Å of coverage. We thus believe that the initial broadening is not related to the formation of a reacted species but more likely to chemisorption-induced perturbation of the charge distribution at the surface.

In Fig. 6 we report attenuation curves  $I(\Theta)/I(0)$  for the Ge 3*d* core emission for  $\Theta \leq 2$  Å based on core EDC's taken at 50- and 75-eV photon energies. Different symbols are for different cleaves and the scatter represents the

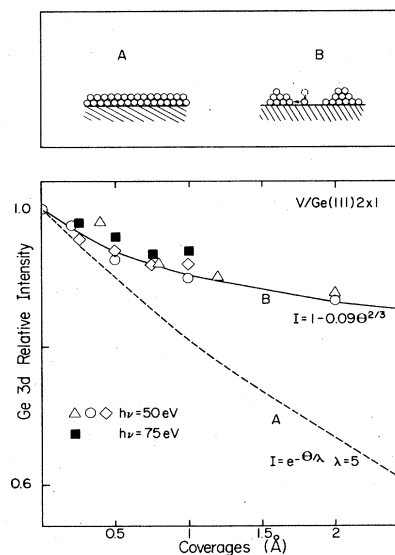


FIG. 6. Attenuation curve for Ge 3*d* in the low-coverage region for two different photon energies ( $h\nu=50$  eV, open symbols;  $h\nu=75$  eV, solid symbols). The scattering is representative of the statistical error. The dashed line represents the exponential attenuation for the model denoted by A in the top model. Model B (island formation) shows good agreement with the experimental results (continuous curve).

statistical error. As shown, the attenuation of the Ge 3d core emission is quite insensitive to variations in the electron escape depth. This is very surprising and is inconsistent with layer-by-layer growth of the sort sketched as type *A*, shown at the top of Fig. 6, since this mode requires exponential variation with escape depth. Assuming a reasonable escape depth of  $\lambda=5$  Å for  $h\nu=75$  eV, we see from the calculated behavior (dashed line labeled *A* in Fig. 6) that layer-by-layer growth cannot explain the experimental data. Instead, if we assume islands which interact with the substrate in the contact area (model *B* in Fig. 6), then we should expect an attenuation of the form  $(1-\alpha\Theta^{2/3})$ . In particular, if we assume that the islands are hemispherical with average radius  $R$  and concentration  $n_c$ , at least in the early stages of nucleation, then  $\alpha$  depends substantially on  $n_c$  and on characteristic parameters of the interface constituent materials, including atomic weight and density. The attenuation takes the form<sup>10</sup>

$$\alpha = \beta \{ 1 + 2\beta R^{-2} [e^{-R/\lambda} (R\lambda + \lambda^2) - \lambda^2] \},$$

where  $\lambda$  is the electron escape depth and  $\beta$  is a function of the already-mentioned parameters. As shown, this model provides very good agreement with the experimental results with  $\alpha=0.09$ . This is consistent with an average island radius  $R \sim 20$  Å at  $\Theta=2$  Å and an average island concentration of  $n_c \sim 10^{12}$  islands/cm<sup>2</sup>. Moreover, once these parameters have been determined, a variation of the escape depth produces a second-order correction for the value of  $\alpha$  (of the order of few percent), in agreement with the experimental results.

Our valence-band results of Figs. 4 and 5 can be interpreted as attenuation of the Ge features and the appearance of V-induced states. Difference curves at 21 eV reveal the growth of new states near the Fermi level about in the position of V 3d emission. No evidence was found in the difference curves for  $\Theta < 2$  Å of the feature denoted by *C* and associated with the formation of the intermixed region. LEED results show, however, that there is no ordered overlayer formation. Indeed, the  $2 \times 1$  LEED pattern for freshly cleaved Ge changes after the deposition of 0.1–2.0 Å in a  $1 \times 1$  pattern, indicating reconstruction of the metastable Ge( $2 \times 1$ ) pattern due to metal adatoms. The LEED pattern fades between 2 and 3 Å into an increasing background. The absence of metal-induced structure seems to indicate that at low coverages a disordered layer is formed. Moreover, the persistence of the ordered substrate pattern to a coverage greater than 2 ML argues against epitaxial growth at room temperature and is consistent with the formation of islands.

This kind of cluster growth ceases at  $\Theta \sim 2$  Å as the clusters become unstable and provide the energy necessary to disrupt the substrate. Fujimori *et al.*<sup>20</sup> have discussed such disruption in terms of the coalescing of islands—or coarsening. Such cluster-induced reactions have been documented recently for Ce/Si.<sup>6</sup> Models involving cluster formation have been proposed recently for some interfaces by Ludeke<sup>3</sup> and by Zunger.<sup>4</sup> Upon disruption, intermixed V-Ge regions are formed, growing along and into the surface as will be discussed in the next section.

## B. Intermediate region

The intermediate region corresponds to coverages between 2 and about 40 Å, where the reaction starts and the overlayer chemistry is fully developed. The morphology of the intermediate region can best be seen through analysis of the core level where each component is considered separately—as can be done with line-shape decomposition of the sort shown in Fig. 2. At the top of Fig. 7

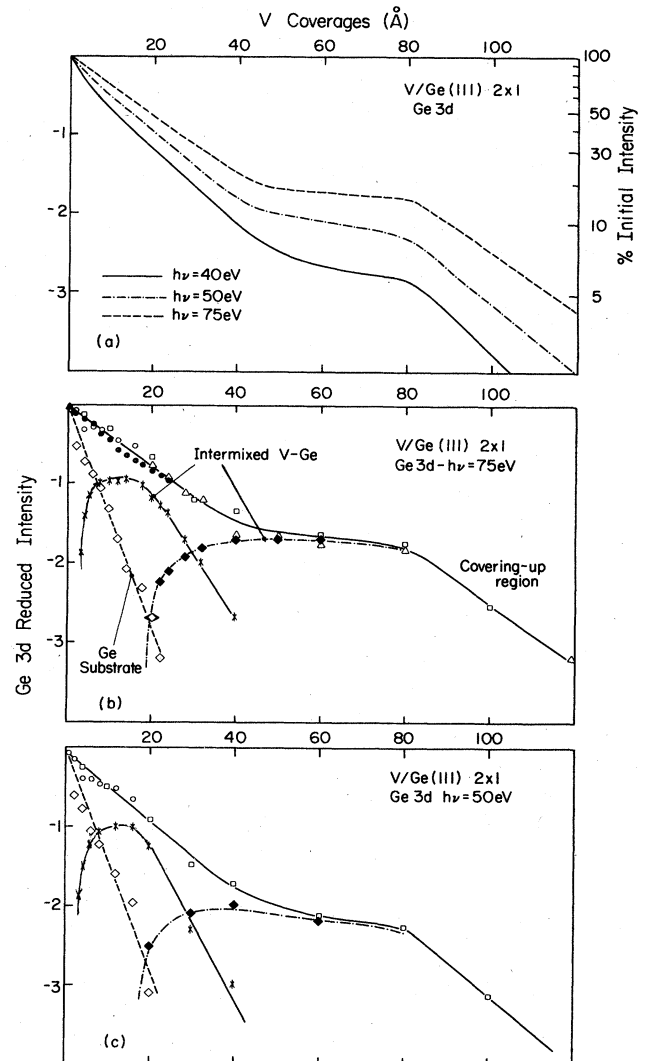


FIG. 7. (a) Relative intensity attenuation curves for photoelectron escape depths of 8–20 Å obtained by varying  $h\nu$ . (b) and (c) Attenuation curves for the Ge 3d core emission. Different symbols correspond to different cleaves. Also shown are results for the growth and/or attenuation curves of the various Ge 3d components based on the line-shape analysis (Fig. 2). The substrate is attenuated with an escape depth of  $\sim 7$  Å. The second species associated with intermixed V/Ge grows to 40% of the initial signal and remains quite constant in the region between 10 and 20 Å. After 20 Å, the segregated species is present and is responsible for the characteristic plateau in the total attenuation curve. Over  $\sim 80$  Å, the interface is covered up with a V film which is increasingly effective as a barrier for Ge out-diffusion.

we plot  $\ln[I_0(\Theta)/I(0)]$  for different photon energies for  $0 < \Theta \leq 120$  Å for the total emission from the Ge 3*d* cores. In the bottom two parts of Fig. 7, we show the growth and/or attenuation for each of the components identified in the line-shape analysis (Fig. 2). From Fig. 7(a) it appears that the total Ge 3*d* core emission is attenuated almost exponentially between 2 and 40 Å with characteristic escape depth of 25, 20, and 16 Å for  $h\nu=75$ , 50, and 40 eV, respectively. This behavior is misleading, however, as can be seen from panels (b) and (c) of Fig. 7. There we can identify and follow the *three* distinct Ge species and see that the Ge-1 substrate emission is exponentially attenuated with a photoelectron escape depth of  $\sim 7$  Å. This is in reasonable agreement with what might be expected for  $h\nu=75$  eV [ $\sim 5$  Å for propagation through crystalline Ge (Ref. 14)].

Once reaction has been triggered at the interface, the component shifted 0.5 eV to lower binding energy grows, reaching a plateau region at  $\sim 8$ -Å coverage with total emission of 38–40% of the initial signal [Fig. 7(b)]. This reacted phase dominates until  $\sim 20$  Å and can be associated with the formation of regions of the intermixed V-Ge phase. The invariance of binding energy of the reacted Ge component indicates that the local chemical environment does not change significantly as the reaction occurs. Changing the photoelectron escape depth within the interface region [10 Å with  $h\nu=50$  eV, Fig. 7(c)] allows us to see that the substrate is still attenuated with the same characteristic length, whereas the Ge-2 phase increases more slowly and reaches 34% of the initial signal at 12 Å. The variation of the plateau value with the escape depth seems to be consistent with the presence of a concentration of  $\sim 40\%$  of Ge in the reacted layer. This number is, however, meaningless and cannot give us the composition of the reacted overlayer without parallel understanding of the growth morphology. Indeed, it is calculated by assuming layer by layer growth—compared to what is most likely heterogeneous growth of the V/Ge interface. Significantly, our results show that a uniformly distributed reacted species is grown, independent of the details of the lateral morphology.

Valence-band results (Figs. 4 and 5) show that the new feature denoted by *C* is present in the intermediate region, appearing first at about 3 Å and becoming well defined between 5 and 20 Å. For  $\Theta \geq 20$  Å, it decreases in intensity and disappears completely by 30 Å. These states can be associated with V—Ge bonds in the intermixed phase. Eventually, they disappear because the intermixed region is covered up by a vanadium layer.

For coverages above 20 Å, a third Ge 3*d* component appears located  $-0.95$  eV lower in binding energy than the bulk component. This component grows and reaches a maximum at 30–40 Å. The results in Fig. 7 show that an apparent strong gradient for this species exists across the film since the Ge-3 signal is reduced by 30% on going from  $h\nu=75$  to  $h\nu=50$  eV and by 60% to 40 eV (7% of the total intensity within the plateau region of the curves). In reality, the relative variation of the escape depth with different photon energies could be altered across the polycrystalline film and could be another reason for the behavior of the attenuation curve. Although we cannot

yet unambiguously describe the distribution of the Ge-3 species across the interface, we can say that this species is related to Ge atoms in a V-rich overlayer. The Ge is, of course, still bonded to vanadium, as shown by the fixed binding energy at which it is located. Similar behavior had been observed for many metal-semiconductor interfaces, including Ce/Si(111) and Cr/GaAs(110).<sup>19</sup>

The valence-band results of Fig. 5 also show that the 20-Å coverage corresponds to a change in the morphology of the interface since a new feature appears at 2.2 eV. Comparison to results for the thick film shows that this is characteristic of a metallic V film. The observed sharpening of the main feature *A* after 20 Å reflects the formation of a V-rich overlayer, consistent with results for Cr/Si (Ref. 10) and Cr/GaAs (Ref. 21).

### C. High-coverage region

The results shown in Fig. 7 reveal that the Ge-3 surface species is dominant for  $\Theta \geq 40$  Å. Between 40 and 80 Å, the concentration of this Ge species is nearly unchanged. For coverages over 80 Å, however, there is an abrupt change in slope of the attenuation curves. From this we conclude that the Ge out-diffusion channels are now much less efficient (but not zero) and the interface is covered up by a thick (polycrystalline) metallic film of vanadium. Note, however, that the rate of attenuation is still far from what one would expect for layer-by-layer covering of the surface. Instead, the intensity of the Ge-3 species drops to 4% of the total Ge 3*d* initial intensity at a coverage of 120 Å ( $h\nu=75$  eV). Finally, we see from the valence-band EDC's of Fig. 5 that convergence to metallic V has occurred.

### D. Schottky-barrier results

The Ge 3*d* core-level spectrum has been measured at  $h\nu=40$  eV with a resolution of  $\sim 300$  meV. This energy is the most bulk sensitive (escape depth  $\sim 15$ –20 Å) available, giving electron kinetic energies of 6.5 eV for the Ge 3*d* core. It is then a good monitor for the variation of the Ge bands induced by metal deposition, considering that after 2 Å the presence of reacted components can make it very difficult to position the substrate doublet for more surface-sensitive results.

The Schottky-barrier height is defined as  $\Phi_b = E_c - E_F$ , where  $E_c$  is the bottom of the conduction band and  $E_F$  is the Fermi level. Variation in band bending implies a rigid shift of all the Ge features, including the core levels. The results reported in Fig. 8 present the relative barrier heights  $\Phi_b - \Phi_b(\text{clean})$  where  $\Phi_b(\text{clean})$  is the reference zero and can be obtained from other measurements. As shown, the interface formation between 0 and 2 Å is responsible for a reduction of the barrier height by 0.125 eV with respect to the original value, previously determined by the pinning of the Fermi level by surface states. As already demonstrated by other workers,<sup>12,22</sup> this final value of  $\Phi_b$  does not depend on the kind of surface assumed as starting point, but is only affected by the bonding at the interface.

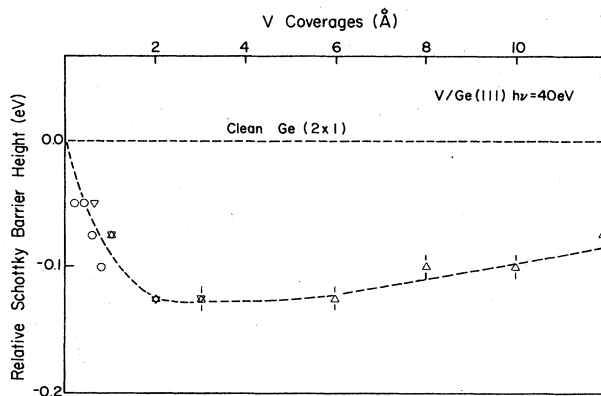


FIG. 8. Changes in the Schottky-barrier height relative to clean Ge(2 $\times$ 1) value with V coverages. The barrier is completely developed by 2 Å. After this point, the trend is reversed.

From Fig. 8 we can see that by 2 Å, when the reaction has started, a slow increase in  $\Phi_b$  is observed. This can be related as a secondary effect to the development of the reacted Ge-2 phase. Indeed, as the reaction proceeds, the interface condition appears to change and a lowering of the Schottky barrier is observed. After 10 Å, it is no longer possible for us to follow this trend due to the increasingly dominant reacted Ge-2 component.

## V. CONCLUSIONS

Our experimental results show that the growth of the V/Ge interface is very complex, but that it can be charac-

terized by dividing the process of the interface formation into several stages which have different growth morphologies and stoichiometries. A first region, in which metal islands nucleate and grow on the surface, is followed by the formation of a thick intermixed layer  $\sim$ 20 ML wide. After 20 Å, the reaction is completed and further metal depositions are accompanied by Ge surface or near-surface segregation up to 80 Å. Finally, the interface is covered with the metal.

It was not long ago that the reactivity of a metal-semiconductor interface was reported by looking only at the deviation of the total core-level attenuation from the layer-by-layer mode. Our work shows how those deviations are related to well-defined stages which occur during the interface formation. Efforts are presently underway to vary the temperature of the interface to enhance and retard reaction and to use other techniques to ultimately create more quantitative models of reacting interfaces.

## ACKNOWLEDGMENTS

This work was supported by the U.S. Office of Naval Research under Grant No. N00014-83-K-0579. The Synchrotron Radiation Center is supported by the National Science Foundation and the assistance of its staff is gratefully acknowledged. Stimulating discussions with R. A. Butera and M. Grioni contributed significantly to this work. J. J. J. is also affiliated with the Materials Science Program, University of Wisconsin, Madison, WI 53706.

- <sup>1</sup>See the recent review by Brillson and its exhaustive citation to the literature [L. J. Brillson, *Surf. Sci. Rep.* **2**, 123 (1982)]. See, also, J. H. Weaver, in *Analysis and Characterization of Thin Films*, edited by K. N. Tu and R. Rosenberg (Academic, New York, in press).
- <sup>2</sup>G. LeLay, *Surf. Sci.* **132**, 169 (1983), reviews noble-metal—elemental-semiconductor interface formation.
- <sup>3</sup>R. Ludeke, *Surf. Sci.* **132**, 143 (1983).
- <sup>4</sup>A. Zunger, *Phys. Rev. B* **24**, 4372 (1981).
- <sup>5</sup>R. R. Daniels, A. D. Katnani, G. Margaritondo, and A. Zunger, *Phys. Rev. Lett.* **47**, 875 (1981).
- <sup>6</sup>M. Grioni, J. J. Joyce, M. del Giudice, D. O'Neill, and J. H. Weaver, *Phys. Rev. B* **30**, 7370 (1984); *Phys. Rev. Lett.* **53**, 2331 (1984).
- <sup>7</sup>R. H. Williams, *Surf. Sci.* **132**, 122 (1983); R. H. Williams, *J. Vac. Sci. Technol.* **18**, 929 (1981).
- <sup>8</sup>Z. Zur, T. C. McGill, and D. L. Smith, *Surf. Sci.* **132**, 456 (1983).
- <sup>9</sup>G. W. Rubloff, *Surf. Sci.* **132**, 268 (1983).
- <sup>10</sup>A. Franciosi, D. J. Peterman, J. H. Weaver, and V. L. Moruzzi, *Phys. Rev. B* **25**, 4981 (1982).
- <sup>11</sup>J. G. Clabes, G. W. Rubloff, and T. Y. Tan, *Phys. Rev. B* **29**, 1540 (1984).
- <sup>12</sup>J. G. Clabes, G. W. Rubloff, B. Reihl, R. J. Purtell, P. S. Ho, A. Zartner, F. J. Himpsel, and D. E. Eastman, *J. Vac. Sci. Technol.* **20**, 684 (1982).
- <sup>13</sup>G. Margaritondo, N. G. Stoffel, and J. H. Weaver, *J. Phys. E*

- 12**, 602 (1979).
- <sup>14</sup>See, for example, I. Lindau and W. E. Spicer, *J. Electron. Spectros. Relat. Phenom.* **3**, 409 (1974); M. P. Seah, *Surf. Sci.* **32**, 703 (1972).
- <sup>15</sup>R. Ludeke, T. C. Chiang, and T. Miller, *J. Vac. Sci. Technol.* **B 1**, 581 (1983).
- <sup>16</sup>J. H. Weaver, C. Krafka, D. W. Lynch, and E. Koch, *Optical Properties of Metals*, Physics Data No. 18-1 and 18-2 (ZAED, Karlsruhe, Germany, 1981). See, also, J. H. Weaver, *CRC Handbook of Chemistry and Physics*, 64th ed., edited by R. C. Weast (CRC, Boca Raton, 1984).
- <sup>17</sup>J. F. Alward, C. Y. Fong, and C. Gupta-Sridhar, *Phys. Rev. B* **18**, 5438 (1978); L. Ley, O. B. Debuosi, S. P. Kowalczyk, F. R. McFeely, and D. A. Shirley, *ibid.* **16**, 5372 (1977).
- <sup>18</sup>L. L. Boyer, D. A. Papaconstantopoulos, and B. M. Klein, *Phys. Rev. B* **15**, 3685 (1977).
- <sup>19</sup>M. Grioni, M. del Giudice, J. J. Joyce, and J. H. Weaver, *J. Vac. Sci. Technol. A* **3**, 918 (1985), discuss of V/GaAs(110).
- <sup>20</sup>A. Fujimori, M. Grioni, and J. H. Weaver [*Phys. Rev. B* (to be published)], discuss the thermochemistry of rare-earth metals on semiconductors and examine island formation.
- <sup>21</sup>J. H. Weaver, M. Grioni, and J. J. Joyce, *Phys. Rev. B* **31**, 5348 (1985), discuss the formation of the Cr/GaAs(110) interface.
- <sup>22</sup>R. Purtell, J. G. Clabes, G. W. Rubloff, P. S. Ho, B. Reihl, and F. J. Himpsel, *J. Vac. Sci. Technol.* **21**, 615 (1982).